Anisotropic magnetic and quadrupolar H-T phase diagram of $CeRh_2As_2$

Burkhard Schmidt and Peter Thalmeier
Max Planck Institute for the Chemical Physics of Solids, D-01187 Dresden, Germany
(Dated: April 17, 2024)

The tetragonal heavy fermion compound $CeRh_2As_2$ has intriguing low temperature symmetry breaking phase whose nature is unclear. The unconventional superconducting phase is complemented by other normal state phases which presumably involve ordering of 4f electron multipoles supported by the Kramers doublets split by the tetragonal CEF. The most striking aspect is the pronounced anisotropic *H-T* phase boundary for in- and out-of plane field direction. Using a localised 4f CEF model we demonstrate that its essential features can be understood as the result of competing low field easy-plane magnetic order and field-induced quadrupolar order of xy- type. We present calculations based on coupled multipole RPA response function approach as well as molecular field treatment in the ordered regime. We use an analytical approach for a reduced quasi-quartet model and numerical calculations for the complete CEF level scheme. We discuss the quantum critical properties as function of multipolar control parameters and explain the origin of a pronounced a-c anisotropy of the *H-T* phase diagram. Finally the field and temperature evolution of multipolar order parameters is derived and the high field phase diagram is predicted.

I. INTRODUCTION

The tetragonal (C_{4v}) compound $CeRh_2As_2$ has been added to the list of heavy fermion systems with complex symmetry breaking phases at low temperature and fields. Primarily superconductivity (SC) was discovered [1] with $T_c = 0.3$ K and proposed [2–4] to be of unconventional nature, in particular for field along c-axis it was suggested that a transition between even and odd parity state takes place in an external field. This transition is claimed to be connected to the lack of local inversion symmetry at the f-electron sites. Furthermore the SC phase was found to be surrounded by other phases which break the symmetry in the normal state [4–7] with a zero-field $T_0 = 0.5\,\mathrm{K}$ which is a familiar scenario for heavy fermion compounds [8]. As for the SC phase what kind of order parameters are involved is still unidentified but μSR experiments suggests that spontaneous magnetic moments are formed below T_0 although their size is still unknown[9]. The magnetic order has been excluded to be of FM type [4, 5] but the ordering wave vector is so far not known, we may conjecture that it is of AF type. Furthermore NMR experiments [10] indicate that magnetism should be of the easy-plane type, judging from spin fluctuations in the disordered phase. Like SC, this unidentified phase appearing below T_0 has, however, a striking a-c axis anisotropy of the phase boundary that seems incompatible with conventional antiferromagnetism. Therefore additional degrees of freedom of 4f electrons have to be involved, a natural candidate are higher order multipoles supported by the Ce^{3+} ($J = 5/2$) CEF states. The latter consist of three Kramers doublets where the lower two may be considered to form a quasi-quartet.

Since $CeRh_2As_2$ is a heavy fermion system hybridization with conduction electrons is present. The estimated Kondo temperature T^* (band width of heavy quasiparticles) is of the same order as the splitting Δ of the quasi-quartet system [5, 11]. However when considering purely the question of symmetry breaking and the stability of multipolar phases the local 4f approach may be a reasonable starting point despite the presence of hybridization. This has been successfully demonstrated for the prominent pure quartet multipole order in CeB_6 [12, 13] and also in the quasi-quartet compound $YbRu_2Ge_2$ [14, 15] which show strong and moderate hybridization effects, respectively. The localized approach will also be used here for $CeRh_2As_2$ to investigate its most striking feature: the extreme anisotropy of the normal state phase diagram. In any case it is necessary to investigate its predictions as a reference point. Recent ARPES experiments [16] have indeed proposed a predominantly localized character of 4f electrons in this compound and support such starting point.

For the determination of the *H-T* phase diagrams we use the reduced quasi-quartet model in an analytical approach as well as the full CEF level scheme with three Kramers doublets in a numerical treatment. From symmetry arguments we identify in which configuration of conjectured dipolar and quadrupolar order parameters one may expect a strong a-c anisotropy of the *H-T* phase diagram to appear. The most convenient technique of its determination is the response function formalism. Starting from the bare single-site CEF level susceptibilities we derive the coupled collective RPA multipole susceptibilities in the external field that include the intersite multipole interactions and follow their singularities from the disordered side which locates the phase boundaries. We show that the coupling of magnetic dipolar and quadrupolar moments happens through mixed multipole field-induced susceptibilities which appear only for the in-plane field direction. The field-induced mixing of the quasi-quartet doublets generates a quadrupolar ground state moment which, through field induced coupling with the dipolar moment stabilizes the ordered phase for the in-plane field. This mechanism is absent for field along c-axis and this distinction lies at the origin of the observed anisotropy of the phase diagram which will be explained in a semi-quantitative way both within the quasi-quartet

model and the full CEF level scheme.

Furthermore we show that at small intersite quadrupolar coupling the AF and field-induced quadrupolar (FIQ) are separated, the former appearing at small the latter at larger fields. As the quadrupole interaction increases at a quantum critical point (QCP) the two phase boundaries approach and rapidly merge into a single phase boundary. We also calculated the field dependence of magnetic and quadrupolar order parameters to illustrate the change of character of the phase diagram as function of interaction control parameters. In addition we comment on the in-plane anisotropy of the QCP fields and their dependence on control parameters. Finally we look at the very high field behavior and show that for the in-plane field the transition temperature of the mostly quadrupolar phase increases up to very large values and then drops steeply when the field strength becomes comparable to the quasi-quartet splitting.

II. THE CEF MODEL FOR $CeRh_2As_2$ AND ITS MULTIPOLE MOMENTS

The complete CEF Hamiltonian model comprising all three doublets appropriate for $J = 5/2$ in C_{4v} site symmetry has been discussed in Ref. 5. It is extended in Appendix A to include the multipolar operators and the dependence of their matrix elements on the CEF mixing parameter θ. The latter has been determined from a fit to the high-temperature susceptibility of $CeRh_2As_2$. It turns out that the level sequence is (energies as temperatures in parentheses) $\Gamma_7^{(1)}$ (0 K, ground state); Γ_6 (30 K) and $\Gamma_7^{(2)}$ (180 K) (we set $k_B \equiv 1$). Therefore at moderate temperatures one has to deal only with a quasi-quartet system consisting of the lowest two doublets split by $\Delta = 30$ K; this restriction is convenient for analytical calculations but fully numerical results comprising all three levels will also be presented. The wave functions of the quasi-quartet are given by $|\Gamma_{7\sigma}^{(1)}\rangle \equiv |1\sigma\rangle$ and $|\Gamma_{6\sigma}\rangle \equiv |2\sigma\rangle$. Their explicit form in terms of free ion 4f states $\{|JM\rangle : M = -J \dots J\}$ are given in Appendix A together with a discussion of the full model comprising three Kramers doublets and its associated multipole operators.

For compelling reasons discussed in Sec. IV we will restrict our model for the order parameters and phase diagrams in $\mathbf{H}_0 \parallel c, a$ to two candidates: The magnetic dipole J_y (choosing external field $\mathbf{H}_0$ along x-axis) and the electric quadrupole $O_{xy} = (J_x J_y + J_y J_x)$ which break and preserve time reversal symmetry, respectively. This model might also be described in a pseudospin language [12, 13] using $\boldsymbol{\sigma} = \pm$ for the Kramers degree of each doublet and $\boldsymbol{\tau} = 1, 2$ for the orbital degree of the two doublets. In order to avoid the various necessary state and operator mappings we here remain in the original basis of total angular momentum operators $\mathbf{J}$.

For the intersite interactions responsible for the possible broken symmetry phases we use the most rudimentary model containing magnetic out-of (c) and in-plane (a) n.n. exchange as well as a n.n quadrupolar interaction. Since both ferromagnetic and ferro-quadrupolar orders are ruled out by experimental evidence the exchange is assumed to be of antiferro-(AF) type for both multipoles. Together with CEF potential and Zeeman term the model is described by

$$\begin{aligned} H = H_{\rm CEF} &- g_J \mu_B \mu_0 \mathbf{H}_0 \cdot \sum_i \mathbf{J}_i \\ &- \frac{1}{2} \sum_{\langle ij \rangle} J_{ij}^c J_i^z J_j^z - \frac{1}{2} \sum_{\langle ij \rangle} J_{ij}^a \left(J_i^x J_j^x + J_i^y J_j^y \right) \\ &- \frac{1}{2} \sum_{\langle ij \rangle} J_{ij}^Q O_{xy}(i) O_{xy}(j) \end{aligned} \tag{1}$$

where we restricted to nearest-neighbor intersite interactions for the multipoles. Here $\mathbf{H}_0$ with index '0' always refers to the *external applied* field whereas later on fields with other indices or none at all ($\mathbf{H}$) refer to the *internal molecular* fields that contain the effect of polarization and spontaneous order. Since we restrict to n.n. $\langle ij \rangle$ sites within the tetragonal plane and the c-axis exchange is subdominant as seen from the susceptibility there are two interaction constants involved: i) the dipolar exchange constant $I_m^0 = z|J_0|$; $(I_m^0 < 0)$ where we suppress a possible a, c exchange anisotropy ii) the quadrupolar effective coupling $I_Q = z|I_0^Q|$; $(I_Q^0 < 0)$ with z denoting the n.n. coordination number. We also define the reduced external field as $\mathbf{h}_0 = g_J \mu_B \mu_0 \mathbf{H}_0$ and later likewise for the reduced molecular field $\mathbf{h}$.

III. THE COUPLED DIPOLAR-QUADRUPOLAR RPA RESPONSE FUNCTIONS

The H-T multipolar phase boundaries which we intend to investigate are most conveniently determined by following the line of singularities for the collective RPA susceptibilities in the H-T plane that marks the onset of long range order. It is also essential to obtain an understanding of the field and temperature dependence of the coexisting magnetic and quadrupolar order parameters inside the ordered region as may be obtained within the molecular field approximation (MFA) discussed in Sec. V.

For nonzero molecular field $\mathbf{H}$ all CEF levels (Kramers doublets) are split leaving only singlets. In this case the static homogeneous single-site (non-interacting) response function for multipole operators X_α acting on the CEF states may be written as

$$\begin{aligned} \chi_{\alpha\beta}^0(T, \mathbf{h}) = &\sum_{n \neq m} \langle n|X_\alpha|m\rangle \langle m|X_\beta|n\rangle \frac{p_n - p_m}{E_m - E_n} \\ &+ \beta \left[\sum_n \langle n|X_\alpha|n\rangle \langle n|X_\beta|n\rangle p_n - \langle X_\alpha\rangle \langle X_\beta\rangle \right] \end{aligned} \tag{2}$$

where the first and second terms are van Vleck and Curie contributions and $\beta = 1/(k_{\rm B}T)$. The energies E_n and states $|n\rangle$ are nondegenerate CEF eigenvalues and eigenstates in the molecular field $\mathbf{h} = \mathbf{h}_0 - I_m\langle J_{x,z}\rangle$ and $p_n = Z^{-1}\exp(-\beta E_n)$ are their thermal occupations with $Z = \sum_n \exp(-\beta E_n)$ denoting the partition function. The notation $\langle X_\alpha\rangle$ denotes the thermal expectation value of the respective operator X_α. In the limit $\mathbf{h} \to 0$ this will also lead to the correct form of the susceptibilities for the three degenerate Kramers doublets.

Now we include inter-site interactions of two different multipoles on nearest-neighbor sites $\langle i,j\rangle$ as defined by $I_{A,B} = \sum_{\langle ij\rangle} I_{A,B}(ij)$. Then the coupled 2×2 multipolar susceptibility matrix in $X_\alpha = (A,B)$ operator space is given by the RPA expression[17]

$$\underline{\chi} = [\underline{1} - \underline{I}\underline{\chi}^0]^{-1}\underline{\chi}^0 \tag{3}$$

where $\underline{I}$ has only the diagonal matrix elements I_A, I_B. The diagonal susceptibility elements of the matrix $\underline{\chi}$ are then obtained as

$$\begin{aligned}
\chi_{AA} &= \frac{\chi^0_{AA}(1 - I_B\chi^0_{BB}) - I_A\chi^0_{AB}\chi^0_{BA}}{1 - I_A\chi^0_{AA} - I_B\chi^0_{BB} + I_AI_B(\chi^0_{AA}\chi^0_{BB} - \chi^0_{AB}\chi^0_{BA})} \\
\chi_{BB} &= \frac{\chi^0_{BB}(1 - I_A\chi^0_{AA}) - I_B\chi^0_{BA}\chi^0_{AB}}{1 - I_A\chi^0_{AA} - I_B\chi^0_{BB} + I_AI_B(\chi^0_{AA}\chi^0_{BB} - \chi^0_{BA}\chi^0_{AB})}
\end{aligned} \tag{4}$$

where we use $I_A = z|I^m_0|$ and $I_B = z|I^Q_0|$. Note that in a non-vanishing field $\mathbf{h}$ the mixed multipole susceptibilities $\chi^0_{BA} = \chi^0_{BA}$ $(A \neq B)$ are generally nonzero, depending on the symmetry of multipole operators. For the current model of three Kramers doublets in $CeRh_2As_2$ we consider the two following relevant cases of coupled dipole (J_y) and quadrupole (O_{xy}) moments as incipient in-plane order parameters. Table I lists the dipoles and quadrupoles and their respective zero-field irreducible representations for point group C_{4v} which can be mutually induced in a finite magnetic field along one of the tetragonal axes. It shows that the most promising case of strong in-/out-of-plane anisotropy is the combination of a Γ_4 quadrupole and an in-plane magnetic Γ_5 dipolar order parameter on which we will focus in the following:
i) out-of-plane field $\mathbf{H}_0 = (0,0,H_0)$ and $A = J_y$ (or equivalently J_x) and $B = O_{xy}$;
ii) in-plane field $\mathbf{H}_0 = (H_0,0,0)$ and $A = J_y$ and $B = O_{xy}$.

In the first case i) we can read off from Table I that the non-diagonal χ^0_{AB} vanishes identically. Then Eq. (4) decouples to

$$\chi_{\alpha\alpha} = \chi^0_{\alpha\alpha}[1 - I_\alpha\chi^0_{\alpha\alpha}]^{-1}, \quad \alpha = A, B \tag{5}$$

for the diagonal components and the field dependences for A, B are mutually independent. In the second case ii) of in-plane field the product J_xH_y belongs to the same C_{4v} representation Γ_4 as O_{xy} and therefore there will be a non-vanishing non-diagonal field-induced susceptibility component $\chi^0_{BA} = \chi^0_{AB}$, consequently the full expressions in Eq. (4) have to be used for the diagonal dipolar and quadrupolar RPA response functions χ_{J_y,J_y} and $\chi_{O_{xy},O_{xy}}$.

IV. RESTRICTED PARAMAGNETIC QUASI-QUARTET MODEL

For understanding the mechanism of dipolar and quadrupolar coexisting order and associated anisotropic phase diagram it is essential to investigate a simplified model which may be treated analytically giving closed solutions for transition temperatures and quantum critical fields. This is possible if we restrict to the lowest two Kramers doublets $\Gamma^{(1)}_7, \Gamma_6$ forming a quasi-quartet in Eq. (A2). In fact if we set the tetragonal CEF parameters like $B^0_2 \to 0$, $B^0_4 \to -B_4$, and $B^4_4 \to -5B_4$ in Eq. (A1), these two doublets would form the cubic Γ_8 quartet for $J = 5/2$. As argued above this interpretation is justified by the small quasi-quartet splitting. It naturally implies that we also restrict to fields and temperatures of the order of the quasi-quartet splitting $\Delta = 30$ K where the upper third quartet is not yet relevant.

A. Essentials of the quasi-quartet model in the field

To study the H-T phase diagram we need to know the split CEF energies and corresponding eigenstates in an applied field. As described in detail in Sec. V it is, however, the molecular fields, generically called $\mathbf{H}$ containing the applied field $\mathbf{H}_0$ *and* the effect of polarization through intersite interactions that acts on each site. In terms of this effective molecular field $\mathbf{H}$ the single site Hamiltonian is given by

$$H = \sum_\Gamma \epsilon_\Gamma|\Gamma\rangle\langle\Gamma| - g_J\mu_{\rm B}\mu_0\mathbf{H}\cdot\hat{\mathbf{n}} \tag{6}$$

where $\epsilon_\Gamma = (-\Delta/2, \Delta/2)$ and $|\Gamma\rangle$ refer to the (shifted) CEF energies and eigenstates of the quasi-quartet consisting of $|1\pm\rangle$ and $|2\pm\rangle$ (Eq. A1). The external field

TABLE I. Dipoles and quadrupoles and their irreducible representations that can be mutually induced by each other in a field along one of the tetragonal axes. The representations refer to zero-field C_{4v} point-group symmetry [18]. Each double-line corresponds to one combination of field direction and dipole component together with their symmetry-compatible quadrupole operator components. See Table IV for a definition of the latter. We note that the fully symmetric O_2^0 cannot be an order parameter since it does not break any local symmetry and therefore is already contained in the CEF Hamiltonian Eq.(A1) of the disordered phase.

(H_x, H_y)		(J_x, J_y)		O_2^0				$O_{x^2-y^2}$		O_{xy}
Γ_5	$\otimes$	Γ_5	$=$	Γ_1	$\oplus$	Γ_2	$\oplus$	Γ_3	$\oplus$	Γ_4
(H_x, H_y)		J_z		(O_{yz}, O_{zx})						
Γ_5	$\otimes$	Γ_2	$=$	Γ_5						
H_z		(J_x, J_y)		(O_{yz}, O_{zx})						
Γ_2	$\otimes$	Γ_5	$=$	Γ_5						
H_z		J_z		O_2^0						
Γ_2	$\otimes$	Γ_2	$=$	Γ_1						

$\mathbf{H}_0$ may be oriented parallel ($\hat{\mathbf{n}} = \hat{\mathbf{x}}$) or perpendicular ($\hat{\mathbf{n}} = \hat{\mathbf{z}}$) to the tetragonal plane, respectively. In the paramagnetic state it is aligned with the molecular field $\mathbf{h} = \mathbf{h}_0 - I_m\langle\mathbf{J}\rangle$. where we defined $\mathbf{h} = g_J\mu_B\mu_0\mathbf{H}$ previously as the reduced field in equivalent energy units; later we will also use the dimensionless field strength $h' = h/\Delta$ normalized to the quasi-quartet splitting.

Out-of-plane case $\mathbf{h} \parallel \hat{\mathbf{z}}$ *(c-axis).* Due to the diagonal J_z matrix the eigenstates will be unchanged but the Kramers doublet ($i = 1, 2$) energies split described by

$$E_{ci}^{\pm} \;=\; (-1)^i\frac{\Delta}{2} \mp m_{ci}h; \quad |E_i^{c\pm}\rangle = |i\pm\rangle. \tag{7}$$

The matrix elements $m_{a,c\,i}^{(\prime)}$ used here and in the following are tabulated in Table III.

In-plane case $\mathbf{h} \parallel \hat{\mathbf{x}}$ *(a-axis).* Now the J_x matrix has nondiagonal elements (Eq. A5), therefore the CEF states will be mixed to new eigenstates. The corresponding mapping onto the new basis may be done by first performing a state rotation inside each doublet and then between the two doublets. The result for the four split level energies is ($i = 1, 2$):

$$\begin{aligned}\tilde{E}_{ai}^{\pm} &= \cos^2\alpha_{\pm}E_{ai}^{\pm} + \sin^2\alpha_{\pm}E_{a\hat{\imath}}^{\pm} \\ &\quad \pm (-1)^i\sin(2\alpha_{\pm})(m_a'h)\end{aligned} \tag{8}$$

where analogous to Eq. (7) $E_{ai}^{\pm} = (-1)^i\frac{\Delta}{2} \mp m_{ai}h$ are the doublets split by their intrinsic linear Zeeman effect. We also used the notation $\hat{\imath} = 2, 1$ for $i = (1, 2)$. The mixing of the two levels is characterized by the angles $\alpha_{\pm}$ according to

$$\tan 2\alpha_{\pm} = \frac{2m_a'h}{\Delta \pm (m_{a2} - m_{a1})h} \to \tan 2\alpha = \frac{2m_a'h}{\Delta} \tag{9}$$

where the approximation holds for $h/\Delta \ll 1$. The eigenstates for the in-plane field are accordingly given by

$$\begin{aligned}|\tilde{E}_{a1}^{\pm}\rangle &= \cos\alpha_{\pm}|E_{a1}^{\pm}\rangle - \sin\alpha_{\pm}|E_{a2}^{\pm}\rangle, \\ |\tilde{E}_{a2}^{\pm}\rangle &= \sin\alpha_{\pm}|E_{a1}^{\pm}\rangle + \cos\alpha_{\pm}|E_{a2}^{\pm}\rangle\end{aligned} \tag{10}$$

with $|E_{ai}^{\pm}\rangle = (|i+\rangle \mp |i-\rangle)/\sqrt{2}$ denoting the individual rotated Kramers doublet states in the transverse field.

For the calculation of the necessary response functions for J_y, O_{xy} one must transform the zero-field multipole operator matrices in Eqs.(A5) and (A7) (the 4×4 block) to the eigenstates in the applied field: i) For c-direction they are unchanged and J_y, O_{xy} are identical to those in Eqs.(A5) and (A7). ii) For a-direction ($\mathbf{H} \parallel \hat{\mathbf{x}}$ chosen) the transformation to the new basis in Eq. (10) leads to

$$J_x = \begin{pmatrix} -M_{a1}^{+} & 0 & -M_{a+}' & 0 \\ 0 & M_{a1}^{-} & 0 & M_{a-}' \\ -M_{a+}' & 0 & -M_{a2}^{+} & 0 \\ 0 & M_{a-}' & 0 & M_{a2}^{-} \end{pmatrix}, \tag{11}$$

$$J_y = \mathrm{i}\begin{pmatrix} 0 & -\tilde{M}_{a1} & 0 & \tilde{M}_{a+}' \\ \tilde{M}_{a1} & 0 & -\tilde{M}_{a-}' & 0 \\ 0 & \tilde{M}_{a-}' & 0 & -\tilde{M}_{a2} \\ -\tilde{M}_{a+}' & 0 & \tilde{M}_{a2} & 0 \end{pmatrix}, \tag{12}$$

$$O_{xy} = \mathrm{i}\begin{pmatrix} 0 & -\tilde{M}_Q & 0 & -\tilde{M}_Q' \\ \tilde{M}_Q & 0 & -\tilde{M}_Q' & 0 \\ 0 & \tilde{M}_Q' & 0 & -\tilde{M}_Q \\ \tilde{M}_Q' & 0 & -\tilde{M}_Q & 0 \end{pmatrix}. \tag{13}$$

Comparing this with the c-axis field $\mathbf{H} \parallel \hat{\mathbf{z}}$ direction in Eqs.(A5) and (A7) we notice that the essential difference are *field-induced* quadrupolar matrix elements $\tilde{M}_Q$ in the split ground state Kramers doublet $\Gamma_7^{(1)}$ which appear for the a-axis field orientation but are absent in the c-axis field direction (because the latter does not mix the CEF eigenstates). Therefore for the latter there will be no mutual dependence of dipole and quadrupole moments in the field whereas for a-axis field direction such a dependence is induced. This distinction is at the origin of the strongly anisotropic behaviour of phase boundaries in the two field directions as derived in detail below.

The other matrix elements for a-axis field are simply modified (or interchanged) as compared to the zero-field case. Explicitly we have for the dipolar operators (with $\hat{\imath} = (2,1)$ for $i = (1,2)$):

$$\begin{aligned} M^{\pm}_{ai} &= m_{ai}\cos^2\alpha + m_{a\hat{\imath}}\sin^2\alpha \mp m'_a \sin 2\alpha, \\ M'_{a\pm} &= m'_a \cos 2\alpha \pm (1/2)(m_{a1} - m_{a2})\sin 2\alpha, \\ \tilde{M}_{ai} &= m_{ai}\cos^2\alpha - m_{a\hat{\imath}}\sin^2\alpha, \\ \tilde{M}'_{a\pm} &= m'_a \pm (1/2)(m_{a1} + m_{a2})\sin(2\alpha) \end{aligned} \tag{14}$$

and likewise for the quadrupolar operator

$$\begin{aligned} \tilde{M}_Q &= m'_Q \sin(2\alpha), \\ \tilde{M}'_Q &= m'_Q \cos(2\alpha). \end{aligned} \tag{15}$$

Importantly the field induced O_{xy} quadrupolar matrix element appears between the same split ground state wave functions as those of the dipolar J_y operator enabling their coupling through mixed response functions. One can see the origin of the induced matrix element directly in the low-field approximation where $\alpha \approx m'_a h/\Delta \ll \pi$. Then $\tilde{M}_{\mathbf{Q}} \approx 2m'_a m'_Q h/\Delta$ which shows that it is linear in h and proportional to *both* magnetic and quadrupolar matrix elements *between* the two doublets. Thus the transverse field mixes a Γ_6 component into the ground state with amplitude $\approx m'_a h/\Delta$ that forms an induced quadrupole ground state moment due to the m'_Q non-diagonal original quadrupole matrix element m'_Q between $\Gamma_7^{(1)}$ lowest and Γ_6 excited CEF Kramers doublet.

B. Response functions in the quasi-quartet system

With the above dipolar and quadrupolar matrices in the molecular field eigenstates we can now compute the bare multipolar response functions in Eq. (2) that enter into the collective RPA susceptibilities in Eq. (4). In this evaluation we assume that the effect of the splitting of upper levels and their thermal occupation may be neglected due to $h/\Delta,\ T/\Delta \ll 1$ and the non-diagonal matrix elements are replaced by their zero-field values, independent of the field direction. However, the split ground state energies, occupations and matrix elements have to be treated exactly. Then we obtain

out-of-plane case $\mathbf{h} \parallel \hat{\mathbf{z}}$ *(c-axis)*:

$$\hat{\chi}^0_{yy} = \hat{\chi}^0_{xx} = \frac{2m'^2_a}{\Delta} + 2m^2_{a1}\frac{\tanh\frac{\hat{\delta}_c}{2T}}{\hat{\delta}_c} \tag{16}$$

where $\hat{\delta}_c = 2m_{c1}h$ is the splitting of the $\Gamma_7^{(1)}$ ground state doublet in the c-parallel field. As explained above for c-parallel field no induced quadrupole moment appears in the ground state and therefore the quadrupolar and mixed dipolar-quadrupolar susceptibilities are very small or vanish, respectively.

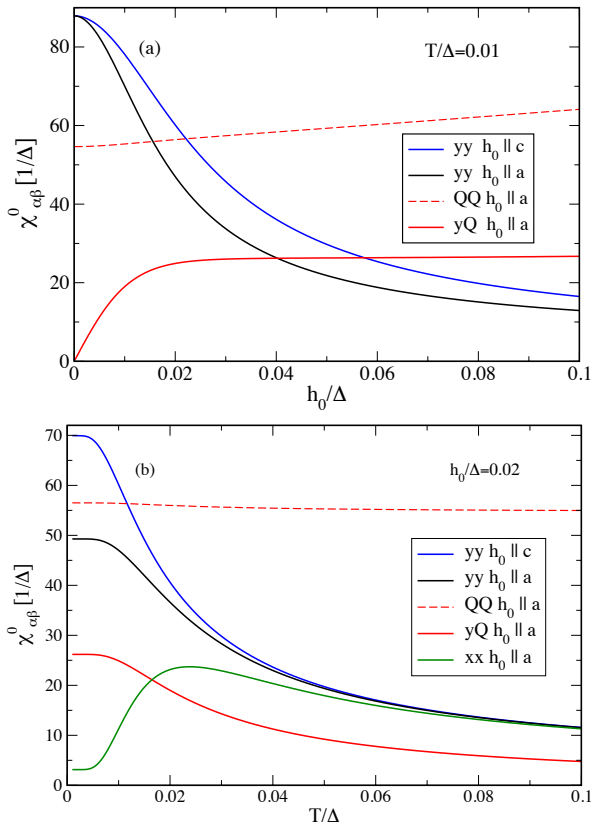

FIG. 1. Bare susceptibilities ($I_m = I_Q = 0$) as function of applied external field h_0 and temperature. (a) The diagonal magnetic susceptibilities are suppressed in the field while the quadrupolar and mixed dipolar/quadrupolar ($\chi_{yQ} \equiv \chi_{Qy}$) ones increase with field. The latter is field-induced, vanishing for $h_0 = 0$. The crossing of χ_{yy} and χ_{yQ} appears in the region of the QCP in Fig. 2. (b) Susceptibilities dominated by pseudo-Curie ground state contribution show strong temperature dependence while the mostly van Vleck quadrupolar one shows very little T-dependence at low fields.

in-plane case $\mathbf{h} \parallel \hat{\mathbf{x}}$ *(a-axis)*:

$$\begin{aligned} \hat{\chi}^0_{yy} &= \frac{2m'^2_a}{\Delta} + \frac{2\tilde{M}^2_{a1}}{\hat{\delta}_a}\tanh\frac{\hat{\delta}_a}{2T}, \\ \hat{\chi}^0_{QQ} &= \frac{2m'^2_a}{\Delta} + \frac{2\tilde{M}^2_{Q}}{\hat{\delta}_a}\tanh\frac{\hat{\delta}_a}{2T}, \\ \hat{\chi}^0_{yQ} &= \left(\frac{2\tilde{M}_a\tilde{M}_Q}{\hat{\delta}_a} + \frac{2m'_a m'_Q}{\Delta}\right)\tanh\frac{\hat{\delta}_a}{2T} \end{aligned} \tag{17}$$

where $\hat{\delta}_a = 2(m_{a1}\cos^2\alpha + m_{a2}\sin^2\alpha)h$ is the ground state doublet splitting in the a-parallel field. The dominant terms in these susceptibilities are the pseudo-Curie terms originating from the split ground state with a splitting energy $\hat{\delta}_a$ and the matrix elements given in Eqs. (14) and (15). The field dependence of these bare response functions is presented in Fig.1 which demonstrates the induced nature of the mixed response $\hat{\chi}^0_{yQ}$.

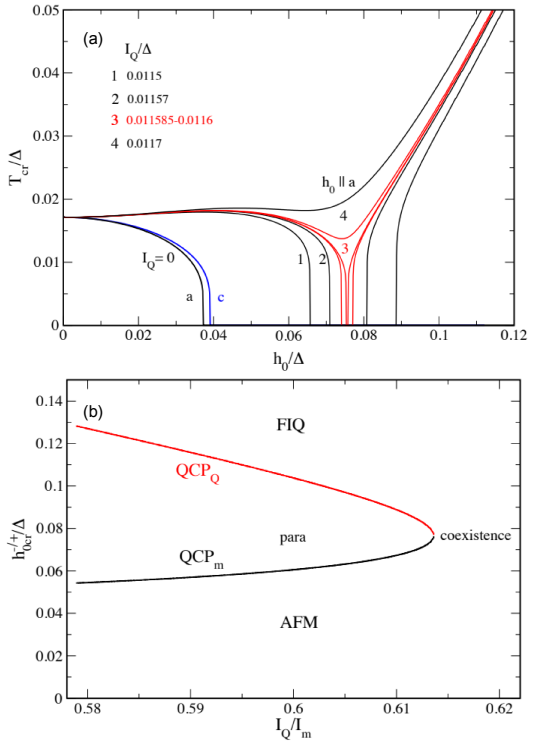

FIG. 2. (a) Low-field phase boundary curves $T_{\rm cr}(h) = T_m$ (left) or T_Q (right) for magnetic exchange $I_m = 0.019$ and various quadrupolar coupling constants I_Q. Note that for $I_Q = 0$ the critical field of AF order for a-direction would be slightly below the value for c-direction. For $I_Q > 0$, however, the former rapidly overtakes the latter while at the same time a new phase boundary appears at higher field that signifies the onset of field-induced quadrupolar (FIQ) order. The two phase boundaries approach each other for increasing I_Q and touch at the QCP defined by Eq. (24). The red curves are for I_Q in the quantum critical region $I_Q \simeq 0.0116$ where (I_m, I_Q) correspond to the dimensionless control parameters $(\xi^m_\Delta, \xi^q_\Delta) \simeq (0.0596, 0.633)$. For even larger I_Q the two separate phase regions merge into one with coexisting AF and FIQ order (see also Fig. 5) for all fields. (b) evolution of QCP lines $h^{\pm}_{0\rm cr}$ for AFM and FQI as function of quadrupolar interaction strength, merging at the QCP endpoint $h_{0\rm cr}$.

C. Phase boundaries in the quasi-quartet model

The transition to the competing multipolar phases for $\mathbf{H}_0 \parallel a$ appears when the RPA susceptibilities in Eq.(4) diverge. This defines the phase boundary in the H-T plane separating the para-phase form the ordered phase with non-vanishing magnetic and quadrupolar order parameters $\langle J_y\rangle$ and $\langle O_{xy}\rangle$ at each site (Sec.V). With $A = J_y$ and $B = O_{xy}$ the singularity appears if the condition

$$\begin{aligned}\mathrm{Det}\left(\underline{1} - \underline{I\chi}^0\right) &= 1 - I_m\chi^0_{yy} - I_Q\chi^0_{QQ} \\ &\quad + I_mI_Q\left(\chi^0_{yy}\chi^0_{QQ} - \chi^0_{yQ}\chi^0_{Qy}\right) \\ &= 0\end{aligned} \tag{18}$$

is met, where $\chi^0_{yQ} = \chi^0_{Qy}$. Using Eq. (17) for the approximate bare susceptibilities this equation may be written in a more transparent form suitable for a closed solution for the critical temperature $T_{\rm cr}(h)$ where the molecular field is given by $h = h_0 - I_m\langle J_x\rangle$. For this purpose we introduce a set of appropriate dimensionless control parameters for dipolar as well as quadrupolar interactions characterized by the magnetic exchange $I_m \equiv I_A$ and quadrupolar $I_Q \equiv I_B$ effective interaction constants, respectively (see after Eqs. (1) and (4)). They are given by

$$\begin{aligned}\xi^m_h &= \frac{2\tilde{M}^2_{a1}I_m}{\hat{\delta}_a}, \quad \xi^m_\Delta = \frac{2m'^2_a I_m}{\Delta}, \\ \xi^Q_h &= \frac{2\tilde{M}^2_Q I_Q}{\hat{\delta}_a}, \quad \xi^Q_\Delta = \frac{2m'^2_Q I_Q}{\Delta}.\end{aligned} \tag{19}$$

The $\xi^{m,Q}_\Delta$ are the control parameters for the non-diagonal van Vleck contributions to the susceptibility while the $\xi^{m,Q}_h$ are those for the pseudo Curie contributions associated with the split ground state doublet. The latter are the more important ones and strongly field dependent. For small fields $h/\Delta \ll 1$ we have $\xi^m_h \sim 1/h$ due to the suppression caused by the splitting while $\xi^Q_h \sim h$ due to the induced quadrupole moment in the split ground state doublet. Hence for increasing field there is a tendency to suppress magnetic order in favor of induced quadrupolar order.

With these expressions the singularity condition Eq. (18) may be expressed as a quadratic equation for $\zeta_a = \tanh(\hat{\delta}_a/2T)$:

$$\begin{aligned}&\bar{\xi}_\Delta(\bar{\xi}_\Delta + 2\bar{\xi}_h)\zeta_a^2 + (\rho_m\xi^Q_h + \rho_Q\xi^m_h)\zeta_a - \rho_m\rho_Q := \\ &A\zeta_a^2 + B\zeta_a - C = 0\end{aligned} \tag{20}$$

where we used the abbreviations $\rho_m = 1 - \xi^m_\Delta$ and $\rho_Q = 1 - \xi^Q_\Delta$. Furthermore we defined the geometric means $\bar{\xi}_\Delta = (\xi^m_\Delta\xi^Q_\Delta)^{\frac{1}{2}}$ and $\bar{\xi}_h = (\xi^m_h\xi^Q_h)^{\frac{1}{2}}$. Then the solutions are $\zeta^\pm_a = [-B + \sqrt{B^2 + 4AC})]/(2A)$. Since $m_{a1} < 0$ also $\hat{\delta} < 0$ and the physical solution is $\zeta^-_a \equiv \zeta_a$. The critical phase boundary is then finally given by

$$T_{\rm cr}(h) = \frac{\hat{\delta}_a(h)}{2\tanh^{-1}\zeta_a(h)} \tag{21}$$

The field dependence of the critical temperature is shown in detail in Fig. 2(a). Thereby the magnetic exchange I_m has been fixed to reproduce the approximate experimental value $T_m(0)/\Delta = 0.017$ and the curves are shown for different quadrupolar interaction parameters. It shows a separation into low field antiferromagnetic (AF) with transition temperature $T_{\rm cr} \equiv T_m(h)$ and high-field field-induced quadrupolar (FIQ) phase (also of staggered type) with transition temperature $T_{\rm cr} \equiv T_Q(h)$. A detailed discussion will be given in Sec. VII.

Here we want to further analyze the quantum critical point (QCP) and surrounding region where the two

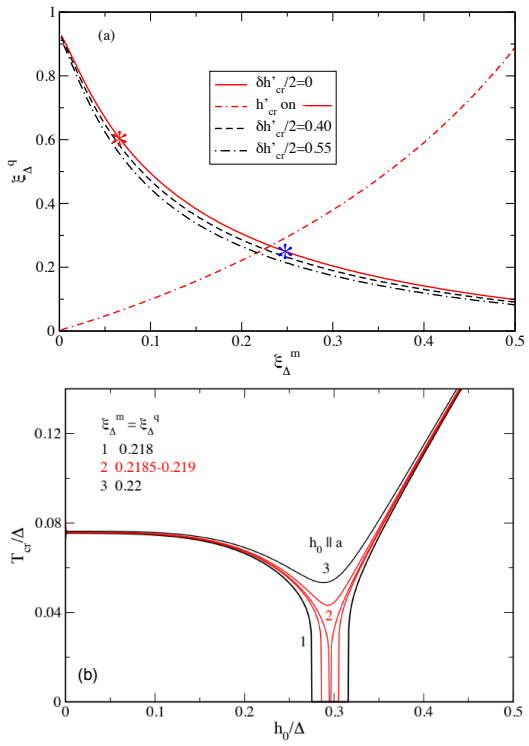

FIG. 3. (a) Contours of constant $\delta h'_{\rm cr}/2$ in the plane of dimensionless control parameters defined in Eq. (19). Along the full red line $\delta h'_{\rm cr}/2 = 0$ the QCP's of AFM and FIQ phases merge to the critical endpoint on the red line. The red and blue stars correspond to the asymmetric interaction parameter case of Fig. 2(a), realised in $CeRh_2As_2$ and to the present (hypothetical) symmetric case in (b), respectively. The red dashed line gives the evolution of the critical field $h'_{\rm cr}$ of the QCP endpoint (i.e.when moving on the red full line). Away from the latter the difference $\delta h'_{\rm cr}$ of the two QCP$_{m,Q}$ critical fields increases rapidly (dashed and dash-dotted black lines) in accordance with Fig. 2(b). In (a) $h'_{\rm cr}$ and $\delta h'_{\rm cr}$ denote molecular fields as given in Eqs. (24) and (25). (b) Critical temperatures as function of applied field for (hypothetical) symmetric case $\xi^m_\Delta = \xi^q_\Delta \simeq 0.22$, cf. Fig. 2(a) for the asymmetrical case of $CeRh_2As_2$.

phases meet and merge into one with coexisting order parameters of both types throughout the whole field range. The zeroes of the transition temperature in Eq. (21) are approached at the two quantum critical fields $h^\pm_{\rm cr}$ when the denominator diverges, i.e. $\zeta_a(h^\pm_{\rm cr}) \to -1$ (negative because $\hat\delta < 0$ due to $m_{a1} < 0$). Their precise values may be read off from Fig. 2(a) obtained from Eqs. (20) and (21) but we also may derive closed expressions for the quantum critical fields. Setting $\zeta_a = -1$ (corresponding to vanishing $T_{\rm cr}$ in Eq. (20)) we arrive at the condition

$$2\bar\xi^2_\Delta - (\rho_m\xi^Q_h + \rho_Q\xi^m_h) + (\xi^m_\Delta + \xi^Q_\Delta) = 1 \qquad (22)$$

In lowest order in $h' = h/\Delta \ll 1$ we find $\xi^m_h = \kappa\xi^m_\Delta/h'$ and $\xi^Q_h = \kappa^{-1}\xi^Q_\Delta h'$, therefore $\bar\xi_h = \bar\xi_\Delta$ independent of h' to this order. Here we defined $\kappa = m_{a1}/(2{m'_a}^2)$ as a measure of the relative strength of diagonal and non-diagonal dipolar matrix elements (Eq. (A7)). The resulting quadratic equation delivers the critical fields of the two QCP's as

$$h'^\pm_{\rm cr} = \tilde B \pm [\tilde B^2 - \tilde C]^{\frac12}$$
$$\tilde B = |\kappa|\frac{\frac12 - (\bar\xi^2_\Delta + \xi^{ar}_\Delta)}{(1-\xi^m_\Delta)\xi^Q_\Delta}, \quad \tilde C = \kappa^2\frac{(1-\xi^Q_\Delta)\xi^m_\Delta}{(1-\xi^m_\Delta)\xi^Q_\Delta} \qquad (23)$$

where in addition to the geometric mean $\bar\xi_\Delta = (\xi^m_\Delta\xi^Q_\Delta)^{\frac12}$ we also use the arithmetic mean $\xi^{ar}_\Delta = \frac12(\xi^m_\Delta + \xi^Q_\Delta)$. From this equation we conclude that two distinct $h^\pm_{\rm cr}$ (QCP_Q and QCP_m in Fig. 2(b)) exist for $\tilde D = \tilde B^2 - \tilde C > 0$ and merge at a unique QCP endpoint for $\tilde D = 0$. For $\tilde D < 0$ the AF and FIQ phases coexist in the whole field range and $h^\pm_{\rm cr}$ no longer appears. We define the *relative* critical field difference of the two phases by the ratio $\delta h'_{\rm cr}/2 = (h'^+_{\rm cr} - h'^-_{\rm cr})/(h'^+_{\rm cr} + h'^-_{\rm cr})$. Then the endpoint is determined by $\delta h'_{\rm cr}/2 = 0$ where explicitly

$$\delta h'_{\rm cr}/2 = \frac{|\kappa|}{(1-\xi^m_\Delta)\xi^Q_\Delta}\tilde D(\xi^m_\Delta, \xi^Q_\Delta)^{\frac12},$$
$$\tilde D(\xi^m_\Delta, \xi^Q_\Delta) = \left[(\bar\xi^2_\Delta + \xi^{av}_\Delta) - \frac12\right]^2 \qquad (24)$$
$$- (1-\xi^m_\Delta)(1-\xi^Q_\Delta)\bar\xi^2_\Delta$$

The condition $\delta h'_{\rm cr}/2 = 0$ defines a quantum critical path in the interaction control parameter plane $(\xi^m_\Delta, \xi^Q_\Delta)$ along which the two QCP's have merged into a single $h'_{\rm cr}$. Along this path its size is given by

$$h'_{\rm cr} = |\kappa|\left(\frac{\xi^m_\Delta(1-\xi^Q_\Delta)}{\xi^Q_\Delta(1-\xi^m_\Delta)}\right)^{\frac12} \qquad (25)$$

Since all our discussion was limited to the small field region, i.e. also $h_{\rm cr} \ll 1$ the above formula is only valid when ξ^m_Δ, $1-\xi^Q_\Delta$ are moderately small. It is nevertheless useful to discuss the limiting cases qualitatively. i) For $(\xi^m_\Delta, \xi^Q_\Delta) \to (0,1)$ $h'_{\rm cr} \to 0$ the magnetic phase vanishes and is replaced by a self-induced quadrupolar phase already at zero field. This is possible because for $\xi^Q_\Delta > 1$ the nondiagonal m'_Q leads to a spontaneous quadrupole order already without field assistance. ii) For $(\xi^m_\Delta, \xi^Q_\Delta) \to (1,0)$ the small quadrupolar control parameter demands a very large field $h'_{\rm cr}$ to reach the merging point with the magnetic transition. This behavior is shown in Fig 3(a) and discussed further in Sec. VII.

We now comment on what one should expect for the in-plane anisotropy of the phase boundaries when the field is rotated perpendicular to c-axis. For a general field direction $\mathbf{h}_0 = (h_{0x}, h_{0y})$ new complications arise: Firstly, two different quadrupoles $(O_{xy}, O_{x^2-y^2})$ can be induced and secondly, together with the dipoles (J_x, J_y) all four multipole operators X_α lead to a full bare susceptibility matrix $\underline{\chi}^0_{\alpha\beta}$ and likewise for the RPA susceptibility matrix $\underline{\chi}_{\alpha\beta}$. The resulting in-plane anisotropy will depend

crucially on the matrix elements and inter-site coupling of the two quadrupoles O_{xy} (m'_Q, I_Q) and $O_{x^2-y^2}$ ($\tilde{m}'_Q, I_{\tilde{Q}}$). It is interesting to consider an extreme case of in-plane anisotropy for $\mathbf{H}_0 \parallel (1,1)$ and $I_{\tilde{Q}} = 0$. Then O_{xy} and $O_{x^2-y^2}$ interchange their roles, i.e. O_{xy} will not be induced and since $I_{\tilde{Q}} = 0$, $O_{x^2-y^2}$ has no effect. Then the lower critical field in Fig.2(a) will be the same as in the a-case (for $I_Q = 0$) and the upper one will not exist, i.e., we would recover the bare magnetic phase diagram for this diagonal field direction.

Finally, in contrast to the in-plane case, the phase boundary for the out-of-plane field $\mathbf{H}_0 \parallel c$ is much simpler to calculate because only the susceptibilities are decoupled according to Eq. (5). Then the singularity for $\chi_{\alpha\alpha}$ ($\alpha = x, y$) simply leads to the magnetic transition temperature

$$T_m^c(h) = \frac{\hat{\delta}_c(h)}{2\tanh^{-1}\frac{1}{\hat{\xi}_h^m}} \tag{26}$$

with the ground state splitting now given by $\hat{\delta}_c(h) = 2m_{c1}h$ and $\hat{\xi}_h^m = \xi_h^m(1-\xi_\Delta^m)^{-1}$ and the c-parallel control parameter is now $\xi_h^m = 2m'^2_a I_m/\hat{\delta}_c$. Furthermore the molecular field is given by $h = h_0 - I_m\langle J_z\rangle$. The resulting critical field is then $h'_{\rm cr} = |m_{c1}|I_m$ formally the same as in the in-plane case T_m^a for $I_Q = 0$. In fact the two $T_m^{a,c}$ (for $I_Q = 0$) are rather similar in Fig. 2(a).

V. DESCRIPTION OF THE ORDERED AF AND FIQ PHASES

Now we turn to a discussion of the ordered phases as characterized by the temperature and field dependence of magnetic and quadrupolar moments using the MFA for the Hamiltonian in Eq. (1). Thereby, in accordance with the n.n. interaction model we assume AF multipole order with sublattices $\lambda = A, B$. The effective single-site Hamiltonian containing three molecular fields to be determined selfconsistently is given by (with $E_0^{\rm mf}(T,H)$ being a constant):

$$H_{\rm MF} \;=\; \sum_{i\lambda} H^\lambda_{\rm MF}(i) + E_0^{\rm mf} \tag{27}$$

For *out-of-plane* field direction ($\mathbf{h}_0 \parallel c$) there can be no induced O_{xy}-type quadrupole and therefore only dipolar molecular fields are present leading to

$$H^\lambda_{\rm mf}(i) \;=\; H_{\rm CEF}(i) - \left[h_z J_z(i) + h^\lambda_y J_y(i)\right] \tag{28}$$

with molecular fields associated with homogeneous polarization $\langle J_z\rangle$ and staggered dipolar order parameter $\langle J_y\rangle_\lambda$ given by (here $\lambda = \pm 1$ for AF sublattices $\lambda = A, B$):

$$\begin{aligned} h_z &= h_0 - I_m\langle J_z\rangle \\ h^\lambda_y &= \lambda h_y;\; h_y = -I_m\langle J_y\rangle \end{aligned} \tag{29}$$

For *in-plane* field direction ($\mathbf{h}_0 \parallel a$) we have a more complex situation with three molecular fields including that of the induced quadrupole:

$$\begin{aligned} H^\lambda_{\rm mf}(i) &= H_{\rm CEF}(i) + H_1(i) \\ H_1(i) &= -\left[h_x J_x(i) + h^\lambda_y J_y(i) + h^\lambda_Q O_{xy}(i)\right] \end{aligned} \tag{30}$$

where the molecular fields corresponding to the in-plane dipolar $\langle J_{x,y}\rangle$ and the induced quadrupolar $\langle O_{xy}\rangle$ are now given by

$$\begin{aligned} h_x &= h_0 - I_m\langle J_x\rangle \\ h^\lambda_y &= \lambda h_y;\; h_y = -I_m\langle J_y\rangle \\ h^\lambda_Q &= \lambda h_Q;\; h_Q = -I_Q\langle O_{xy}\rangle \end{aligned} \tag{31}$$

We stress again that h_0 is the external field and fields with any other index or none at all (h) are molecular fields. It is those that are determined from the self-consistency equations. Then calculating the polarizations $\langle J_z\rangle$ or $\langle J_x\rangle$ for the obtained molecular fields the external field corresponding to the selfconsistent set of molecular field may be obtained from the first of the equations in Eqs. (29) and (31). From the eigenvalues E_n and eigenstates $|n,\lambda\rangle$ of this Hamiltonian that depend on the three expectation values the latter have to be determined selfconsistently according to $\langle A\rangle_\lambda = \sum_{\rm n} {\rm p_n}\langle {\rm n}\lambda|{\rm A}|{\rm n}\lambda\rangle$. Now $p_n = Z^{-1}\exp(-E_n/T)$ are the occupation of (fully split) CEF levels in the molecular fields with $Z = \sum_n \exp(-E_n/T)$ denoting their MF partition function. Using the above equations the temperature and field dependence of $\langle J_x\rangle$, $\langle J_y\rangle_\lambda = \lambda\langle J_y\rangle$ and $\langle O_{xy}\rangle_\lambda = \lambda\langle O_{xy}\rangle$ may be calculated numerically using the full CEF level scheme. For the purpose of deeper understanding of field induced polarization and mutual competition of order parameters it is, however, useful to investigate again the quasi quartet model within an analytical approach for the ordered phases.

A. Order parameters, polarizations and effective molecular fields, effective operator treatment

The staggered order parameters and homogeneous polarizations in Eqs. (29) and (31) may be obtained analytically by restricting to the quasi-quartet model in the limit $h, T \ll \Delta$. We focus mainly on the most interesting case where competing order parameters exist:

For *out-of-plane* field direction ($\mathbf{h}_0 \parallel a$) the calculation is rather involved due to the presence of the induced quadrupolar order parameter $\langle O_{xy}\rangle$. In the quasi-quartet space the MF Hamiltonian is given explicitly by a 4×4 matrix that has now entries at all places:

$$H^\lambda_{\rm MF} = \begin{pmatrix} -\frac{\Delta}{2} & -m_{a1}h^\lambda_- & im'_Q h^\lambda_Q & -m'_a h^\lambda_+ \\ -m_{a1}h^\lambda_+ & -\frac{\Delta}{2} & -m'_a h^\lambda_- & -im'_Q h^\lambda_Q \\ -im_Q h^\lambda_Q & -m'_a h^\lambda_+ & \frac{\Delta}{2} & -m_{a2}h^\lambda_- \\ -m'_a h^\lambda_- & im'_Q h^\lambda_Q & -m_{a2}h^\lambda_+ & \frac{\Delta}{2} \end{pmatrix} \tag{32}$$

where we defined the complex MF expressions $h^\lambda_\pm = h_x \pm i\lambda h_y$. Unlike for the paramagnetic case of Eq. (6) the eigenvalues and -states of this MF Hamiltonian can no longer be obtained analytically. Therefore we resort to the effective operator technique [19] where, due to $h/\Delta \ll 1$ the effect of the upper Γ_6 doublet is eliminated and incorporated in an effective ground state Hamiltonian whose energies and eigenstates can be computed analytically and likewise the dressed matrix elements of multipole operators in the split ground state doublets are obtained. This procedure, based on Brillouin-Wigner perturbation theory, leads to

$$\begin{aligned} H^\lambda_{\rm eff} &= \begin{pmatrix} -\frac{\Delta^*}{2} & \frac{\hat\delta_\lambda}{2} \\ \frac{\hat\delta^*_\lambda}{2} & -\frac{\Delta^*}{2} \end{pmatrix}, \quad -\frac{\hat\delta_\lambda}{2} = \frac{1}{2}(\hat\delta_1 + i\lambda\hat\delta_2), \\ \hat\delta_1 &= -2\left(m_{a1}h_x + \frac{2}{\Delta}m'_a m'_Q h_y h_Q\right), \\ \hat\delta_2 &= \lambda 2\left(m_{a1}h_y + \frac{2}{\Delta}m'_a m'_Q h_x h_Q\right) \end{aligned} \tag{33}$$

The diagonal element $-\Delta^*/2$ is a renormalised level position that plays no role, The effective MF energy levels E_n $(n = \pm)$, shifted by $\frac{\Delta^*}{2}$ of the split $\Gamma_7^{(1)}$ ground state are then given by

$$E_\pm = \mp\frac{1}{2}|\hat\delta| = \mp\frac{1}{2}(\hat\delta_1^2 + \hat\delta_2^2)^{\frac{1}{2}} \tag{34}$$

independent of sublattice $\lambda = A, B$. The corresponding eigenstates $|\psi_{n\lambda}\rangle$ $(n = \pm)$ in the basis of the unperturbed $|1\pm\rangle$ doublet states are represented by the columns of the unitary matrix

$$U^\dagger_\lambda = \frac{1}{\sqrt{2}}\begin{pmatrix} 1 & e^{i\lambda\phi} \\ -e^{-i\lambda\phi} & 1 \end{pmatrix}, \quad \tan\phi = \hat\delta_2/\hat\delta_1 \tag{35}$$

For the calculation of order parameters we still need the diagonal elements of multipole operators within these eigenstates that contain the admixture effects with the upper Γ_6 levels. For an operator $A = \mathrm{J_x}, \mathrm{J_y}, \mathrm{O_{xy}}$ this is achieved by defining the dressed operator $\mathcal{A}_{\rm eff}$ (H_1 is defined in Eq.(30)):

$$\begin{aligned} &\langle k|\mathcal{A}_{\rm eff}|\mathrm{l}\rangle = \\ &\quad A_{\rm kl} - \frac{1}{\Delta}\sum_\mu \left[\langle \mathrm{k}|\mathrm{H_1}|\mu\rangle\langle\mu|\mathrm{A}|\mathrm{l}\rangle + \langle \mathrm{k}|\mathrm{A}|\mu\rangle\langle\mu|\mathrm{H_1}|\mathrm{l}\rangle\right] \end{aligned} \tag{36}$$

where k, l runs over the unperturbed $|1\pm\rangle$ ground state doublet and μ over the unperturbed $|2\pm\rangle$ excited doublet states. The diagonal matrix elements in the split ground state doublet of the MF effective Hamiltonian are then given by

$$\langle\psi_{n\lambda}|A|\psi_{\mathrm{n}\lambda}\rangle = \sum_{\rm kl}\mathrm{U^{\lambda *}_{nk}U^\lambda_{nl}}\langle \mathrm{k}|\mathcal{A}_{\rm eff}|\mathrm{l}\rangle = \mathrm{tr(W^\lambda_n\mathcal{A}_{\rm eff})} \tag{37}$$

where we defined the Hermitian matrix $\{W^{\lambda *}_n\}_{kl} = U^*_{nk}U_{nl} = \{W^\lambda_n\}_{lk}$ or explicitly $(n = \pm)$

$$W^\lambda_n = \frac{1}{2}\begin{pmatrix} 1 & -ne^{i\lambda\phi} \\ -ne^{-i\lambda\phi} & 1 \end{pmatrix} \tag{38}$$

Using the above set of equations the MF expectation values in the case $t, h \ll \Delta$ may finally be calculated as

$$\begin{aligned} \langle J_x\rangle &= \left[-m_{a1}\cos\phi + \frac{2}{\Delta}m'_a m'_Q h_Q \sin\phi\right]\tanh\frac{|\hat\delta|}{2T} + \frac{2}{\Delta}{m'_a}^2 h_x, \\ \langle J_y\rangle_\lambda &= -\lambda\left[-m_{a1}\sin\phi + \frac{2}{\Delta}m'_a m'_Q h_Q \cos\phi\right]\tanh\frac{|\hat\delta|}{2T} + \lambda\frac{2}{\Delta}{m'_a}^2 h_y, \\ \langle O_{xy}\rangle_\lambda &= \lambda\left[\frac{2}{\Delta}m'_a m'_Q(h_x\sin\phi - h_y\cos\phi)\right]\tanh\frac{|\hat\delta|}{2T} + \lambda\frac{2}{\Delta}{m'_Q}^2 h_Q. \end{aligned} \tag{39}$$

With the molecular fields given in Eq.(31) this closed set of equations for the homogeneous polarization and the two staggered order parameters then has to be solved numerically. They have been written in a form to make their physical content transparent: i) In each operator expectation value the last term is due to the direct admixture of the the excited Γ_6 into the ground state $\Gamma_7^{(1)}$ by the molecular field connected with the *same* operator. ii) For $\langle J_x\rangle$ and $\langle J_y\rangle$ the first terms in parentheses are due to the direct contribution of the $\Gamma_7^{(1)}$ ground state to the expectation value. There is no such term for the quadrupolar $\langle O_{xy}\rangle$ order parameter since this operator has no (bare) matrix elements in the Kramers doublet ground state (Eq. (A7)). iii) For $\langle J_x\rangle$ and $\langle J_y\rangle$ the second and for $\langle O_{xy}\rangle$ the only term in parentheses are due to induced matrix elements in the $\Gamma_7^{(1)}$ ground state caused by the *complementary* molecular field, i.e. quadrupolar h_Q for the former and dipolar h_x, h_y for the latter. This term leads to the mutual influence and competition of order parameters. It is also useful to check the purely

magnetic case setting $I_Q = h_Q = 0$. Then we obtain

$$\begin{aligned}\langle J_x\rangle &= -m_{a1}\cos\phi\tanh\frac{\hat{\delta}}{2T} + \frac{2}{\Delta}{m'_a}^2 h_x,\\ \langle J_y\rangle_\lambda &= \lambda m_{a1}\sin\phi\tanh\frac{\hat{\delta}}{2T} + \frac{2}{\Delta}{m'_a}^2 h_y,\end{aligned} \tag{40}$$

where now we have the simplified $|\hat{\delta}| = 2|m_{a1}|(h_x^2+h_y^2)^{\frac{1}{2}}$ and $\tan\phi = -(h_y/h_x)$ without the $\sim h_Q$ contributions.

In the paramagnetic state with $\phi = 0$ and $\langle J_y\rangle_\lambda = 0$ only the homogeneous polarization survives and is given by

$$\begin{aligned}\mathbf{h}_0 \parallel a : \langle J_x\rangle &= m_{a1}\tanh\frac{2m_{a1}h_x}{2T} + \frac{2}{\Delta}{m'}^2_a h_x,\\ &\to |m_{a1}| + \frac{2{m'}^2_a}{\Delta}h_a,\\ \mathbf{h}_0 \parallel c : \langle J_z\rangle &= m_{c1}\tanh\frac{2m_{c1}h_z}{2T} \to |m_{c1}|,\end{aligned} \tag{41}$$

and the corresponding molecular fields are given by $h_{x,z} = h_0 - I_m\langle J_{x,z}\rangle$. Here the arrows imply the zero-temperature limit.

VI. NUMERICAL TREATMENT OF $CeRh_2As_2$ WITH FULL CEF LEVEL SCHEME

The numerical evaluation of the RPA equations starting from Eqs. (2) is in principle identical to the treatment of the quasi-quartet in the preceding sections, however this time involving all six crystal-field states of the $J = 5/2$ multiplet. This is important as soon as temperatures and/or applied magnetic fields cannot be regarded as small compared to the CEF level splittings, in particular to Δ.

We start with Eq. (3) as before. The general form of the bare susceptibility $\chi^0_{AB} = \chi^{\rm vV}_{AB} + \chi^{\rm C}_{AB}$ we use is

$$\begin{aligned}\chi^{\rm vV}_{AB} &= \mathrm{Tr}\left[M(A,B)\cdot D\right],\\ \chi^{\rm C}_{AB} &= \beta\left\{\mathrm{Tr}\left[M(A,B)\cdot P\right]\right.\\ &\quad\left. - \mathrm{Tr}\left[N(A)\cdot P\right]\mathrm{Tr}\left[N(B)\cdot P\right]\right\}.\end{aligned} \tag{42}$$

For the respective components we use indices m, n to label the CEF states and define $(2J+1 = 6)$-dimensional matrices

$$\begin{aligned}M(A,B) &= (m_{mn}(A,B)),\\ m_{mn}(A,B) &= \langle m\,|A|\,n\rangle\,\langle n\,|B|\,m\rangle,\\ D &= (d_{mn}),\\ d_{mn} &= \frac{p_m - p_n}{E_n - E_m}\left[1 - \delta(E_n - E_m)\right],\\ N(A) &= (n_{mn}(A)),\\ n_{mn}(A) &= \langle m\,|A|\,n\rangle,\\ P &= (p_{mn}),\\ p_{mn} &:= p_m\delta(E_n - E_m),\\ p_m &:= \frac{1}{Z}\mathrm{e}^{-\beta E_m},\quad Z := \sum_n \mathrm{e}^{-\beta E_n}\end{aligned} \tag{43}$$

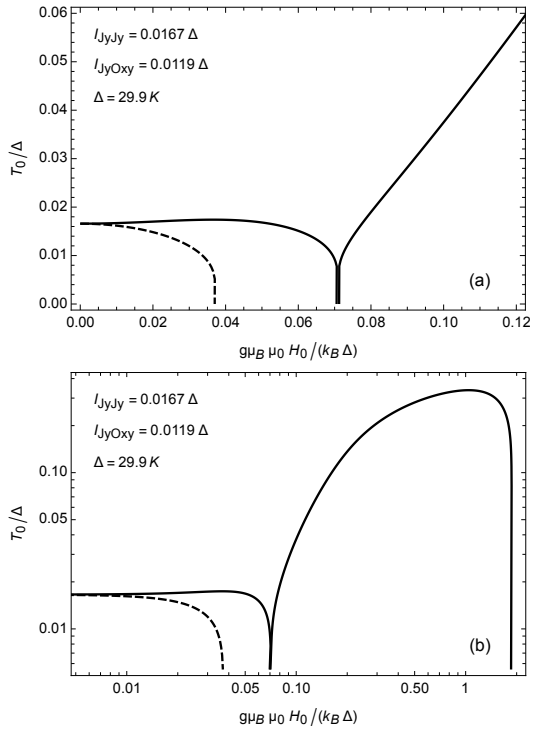

FIG. 4. Phase boundary plot for $\mathbf{H}_0 \parallel$ a as obtained from numerical calculations for the full $J = 5/2$ CEF level scheme with three Kramers doublets at $0, 30, 180$ K. (a) low field regime (cf. Fig. 2(a). (b) full field range in log-log plot. The maximum corresponds to $T_{\rm cr} \simeq 0.3\Delta$ at $h_0/\Delta \simeq 1$. The CEF parameters (Appendix A) are taken from experiment.[5]

where the expression $\langle m|A|n\rangle$ denotes a matrix element of an operator A between states $|m\rangle$ and $n\rangle$ for finite molecular field $\mathbf{h}$. Here we replace the notion of "diagonality" with "energy equality" to avoid numerical issues not only at zero field (Kramers doublets) but rather also at large applied fields when the Zeeman splitting is of the order of the crystal-field splitting.

To determine the RPA phase boundary $T_{\rm cr}(h)$ we use the secular equation equivalent to Eq. (18). Coming from the paramagnetic side, h is the total molecular field in either the x direction or the z direction, respectively. Therefore, as a second step, we have to determine the applied field through $h_0 = h + I_m\langle J_\alpha\rangle$ where $\alpha = x$ or z depending on the field direction, see also Eqs. (31). Here the angular brackets denote the thermal expectation value calculated as the average over the statistical operator of the mean-field Hamiltonian. Fig. 4 shows the two phase boundaries for $\mathbf{h}_0$ parallel to x (solid line) and z (dashed line) determined in this way for one particular choice of parameters closely resembling the low-field results of the quasiquartet model in Fig. 2(a) and the experimental situation in $CeRh_2As_2$ [4, 5]. A further discussion is given below.

VII. DISCUSSION OF NUMERICAL RESULTS

We start our discussion with the field and temperature behavior of the bare susceptibilities $\chi^0_{\alpha\beta}$ without intersite interactions shown in Fig. 1. The rapid reduction of dipolar components in the field (a) is due to the ground state splitting which suppresses their dominant Curie terms. The reduction is stronger for a- than for c- direction because $|m_{a1}| > |m_{c1}|$ (Table III). The quadrupolar susceptibility which has no ground-state contribution for zero field is almost constant due to the dominant van Vleck term controlled by m'_Q. The most important aspect is the rapid field-induced increase of mixed χ^0_{yQ} susceptibilities which are allowed by symmetry, in contrast to χ^0_{xQ} which remains zero. The decrease of dipolar components and increase of the mixed χ^0_{yQ} suppresses the magnetic and favors quadrupolar the quadrupolar instability obtained from the interacting RPA susceptibilities in Eqs. (3) and (4). The complementary temperature dependence is shown in (b) with the expected decrease caused by the reduction of thermal population difference in the split ground state doublet. While yy, zz remain finite the xx component is reduced to zero at low temperatures; the latter plays no role in the ordering instabilities.

The location of instabilities defines the H-T phase diagram of the model for $CeRh_2As_2$, i.e. the critical field curves $T_{\rm cr}(H_0, T)$ which are presented in Fig. 2 based on the analytical calculation (Eq. (21)) for the quasi-quartet model. The magnetic exchange coupling I_m is fixed such that $T_{\rm cr}(0)/\Delta = 0.017$ corresponding to the experimental value [5].For absent quadrupolar coupling the magnetic $T_{\rm cr}(H_0) = T_m(H_0)$ transition temperature behaves quite similar for both field directions. For c-direction it is slightly larger than for a-direction because as explained above the bare susceptibilities are also slightly larger for the former case.

The near *a-c isotropy* of the magnetic phase diagram for $I_Q = 0$ means that the observed [4, 5] strong *a-c anisotropy* in $CeRh_2As_2$ demands the inclusion of other multipoles and their interaction beyond the purely magnetic dipoles. There are many examples in 4f compounds where this has also been observed like, e.g. Rare-Earth hexaborides [13], 4f-skutterudites [20] and Yb-compounds [14, 15, 21]. As we have argued before the field induced coupling to the O_{xy} quadrupole with its strong non-diagonal matrix element and resulting large bare and field-induced susceptibilities (Fig. 1) is a prime candidate. The effect of this inclusion on the critical field curves as function of the O_{xy} intersite coupling strength is immediately seen in Fig. 2(a) as a strong *increase* of the (lower, AF) critical field $h^-_{0\rm cr}$ with I_Q and the concomitant appearance of a second transition at higher critical field $h^+_{0\rm cr}$ which *decreases* with increasing I_Q and represents a phase with primary quadrupolar order. For $h^-_{0\rm cr} < h < h^-_{0\rm cr}$ one has again a sector with fully disordered phase. Since the two values $h^\pm_{0\rm cr}$ characterizing the $\mathrm{QCP}_{m,Q}$ for the two order parameters move into opposite directions with increasing I_Q this means that at a critical value of I_Q the two critical field curves will touch and merge into one curve (the red curves in Fig. 2(a)) , i.e., the disordered sector vanishes at a QCP endpoint and one has coexisting AF and quadrupolar order throughout the field range $h \ll \Delta$ where the quasi-quartet model is applicable. Actually this does not change qualitatively when performing the numerical calculations for the full model comprising all CEF states as discussed below. The opposite movement of the $\mathrm{QCP}_{m,Q}$ fields with quadrupolar coupling is presented separately in Fig. 2(b) and it clearly demonstrates the merging in a quantum critical endpoint at around $I_Q \simeq 0.0116$. The real phase diagram in $CeRh_2As_2$ is qualitatively well described by our theoretical results close to the QCP endpoint: An observed phase line with almost constant $T_{\rm cr} = T_m$, intercepted by a perpendicular phase boundary and after this a strong, almost linear increase of $T_{\rm cr} = T_Q$ with field. The behavior of the magnetic and quadrupolar order parameters in the various sectors of the phase diagram will be discussed below.

It is worthwhile to avert the discussion of $CeRh_2As_2$ for a moment in favor of a more general perspective. It is interesting to follow the structure of the phase diagram and its segmentation as function of *both* interaction parameters, magnetic I_m as well as quadrupolar I_Q or better in terms of their associated dimensionless control parameters ξ^m_Δ and ξ^Q_Δ. This is presented in Fig. 3(a). It shows the line of QCP endpoints in the plane of control parameters that separates the coexistence phase with merged critical field lines from the region where two separate QCP_m and QCP_Q still exist. The contours correspond to the magnitude of the critical field splitting given in Eq. (24). On the (full) QCP endpoint line the asymmetric values $(\xi^m_\Delta, \xi^Q_\Delta) \simeq (0.059, 0.633)$ correspond approximately to $CeRh_2As_2$. But the same qualitative phase diagram with touching critical field curves would be obtained with more symmetric control parameters $(\xi^m_\Delta, \xi^Q_\Delta) \simeq (0.219, 0.219)$ as shown in Fig. 3(b). In this case, however, the size of $T_{\rm cr}(0)$ and $h_{0\rm cr}$ with respect to CEF splitting Δ have increased by a significant factor as compared to the asymmetric case of $CeRh_2As_2$(Fig.2(a)).

We now turn to the question to which extent the low-field approximation for the quasi-quartet agrees with the all-numerical calculation for the full level scheme including three Kramers doublets, This calculation is valid for any field strength and it is interesting to follow $T_{\rm cr}$ to find out its possible maximum $T^a_{\rm max}$ and corresponding maximum field $h^a_{0\rm max}$ as well as the upper critical field $h^a_{0\rm cr'}$ which should occur when the Zeeman splitting becomes comparable to Δ and homogeneous field polarization overwhelms the staggered order. First we show again the low field regime in Fig. 4(a). It agrees well qualitatively with the quasi-quartet results in Fig. 2(a) with only minor numerical differences of critical field and quadrupolar interaction parameters. The extension to high fields is shown in a double logarithmic plot in

TABLE II. Summary of critical and maximum quantities (units: $\Delta = 30$ K ,T or K) obtained from the the theoretical results in Fig. 4 together with two critical fields from experiments in $CeRh_2As_2$[4, 5]. The reduction factor (last column) is evidence of the Kondo screening of moments and of similar size for both directions.

critical/extremal quantity	CEF-RPA calculation	experiment	ratio
$h^c_{0\mathrm{cr}}$	$0.0375 \equiv 1.95$ T	$6-7$ T	0.33
$h^a_{0\mathrm{cr}}$	$0.071 \equiv 3.69$ T	9 T	0.41
$h^a_{0\mathrm{max}}$	$1 \equiv 52.11$ T	–	–
T^a_{max}	$0.34 \equiv 10.2$ K	–	–
$h^a_{0\mathrm{cr}'}$	$1.95 \equiv 96.40$; T	–	–

Fig. 4(b). It demonstrates that the maximum occurs at $T_{\mathrm{cr}}(h^a_{0\mathrm{max}}) = T^a_{\mathrm{max}} \simeq 0.34\Delta$ for $h^a_{0\mathrm{max}} \simeq \Delta$ which is in the expected range. The very large increase of T_{cr} of the induced quadrupolar phase compared to the zero field value of the magnetic phase is due to the large ratio of matrix elements m'_Q/m_{a1}.

At this point it is appropriate to estimate the absolute magnitude of critical fields, temperatures and magnetic moment in view of partly known experimental quantities. We have shown already that the anisotropy and other basic features of the calculated magnetic and quadrupolar phase diagram reproduces the empirical findings in Refs.4 and 5 and others. It must be said from the outset, however, that one cannot expect a quantitative agreement since we used a purely localized 4f electron approach. In reality the Kondo screening will have a large influence on the magnetic properties. This can be directly seen from the ordered moment $\mu = g_J\mu_{\mathrm{B}}\langle J_\alpha\rangle_0$; $(\alpha = x, z; g_J = 6/7)$ with the saturation order parameter (Eq. (41)) $\langle J_\alpha\rangle_0 = 0.97$ we have $\mu = 0.83\mu_B$. There are no experiments yet that have identified an ordered moment but one should expect a strong reduction of the size of the moment due to Kondo screening known also from other magnetically ordered heavy fermion compounds. This may be concluded from the fact that the Kondo scale T^* has been reported [5] to be of the same order of magnitude as the CEF splitting Δ. Using the scaling factor $(g_J\mu_B)/\Delta = 0.0192T^{-1}$ we obtain critical/maximum field and temperature values that are compared to the know experimental values in Table II. It shows that the theoretical critical field values are lower than the experimental ones which may again be attributed to the large unscreened moments in the localized picture resulting in a too large Zeeman effect. The Table II. shows that the maximum quadrupolar ordering temperature reached at $H^a_{0\mathrm{max}} = 52$ T is $T^{\mathrm{max}}_{\mathrm{cr}} = 10.2$ K and the upper critical field $H^a_{0\mathrm{cr}'} = 96$ T where induced quadrupole order is finally destroyed. These exceptionally enhanced values have not yet been identified in $CeRh_2As_2$. We note, however, that similar values are known from a related compound with quadrupolar order, the cubic, genuine Γ_8 quartet system CeB_6[12, 13, 22] which shows quadrupolar order already in zero field (and induced octupole at finite field) due to the absence of splitting in cubic symmetry. It has maximum values observed in pulsed-field experiments at (40 T, 10 K) and a upper critical field estimated to be 80 T [22, 23]. Thus the theoretical values obtained here in the localized 4f-electron approach may well give a realistic estimate in particular since the influence of Kondo screening is strongly reduced at such high fields.

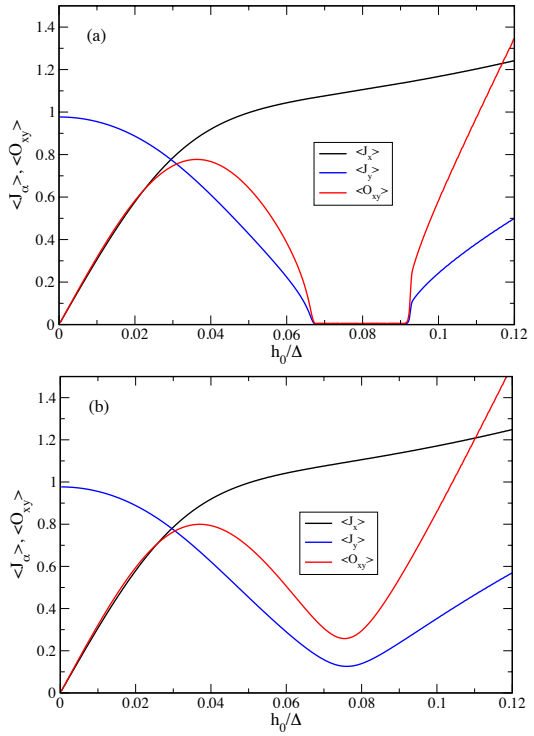

FIG. 5. Dependence of homogeneous polarisation $\langle J_x\rangle$ and order parameters $\langle J_y\rangle, \langle O_{xy}\rangle$ on the applied field. (a) For $I_m = 0.019, I_Q = 0.01157$ in the region with separated AFM/FIQ phases and intervening para-phase. On the upper critical field $h^+_{0\mathrm{cr}}$ the order parameters show a first-order type jump to finite value. (b) For $I_m = 0.019, I_Q = 0.0117$ within merged coexistence phase. In both cases $T/\Delta = 0.005$. For intermediate I_Q corresponding to QCP endpoint see Fig. 6.

Now finally we want to discuss to the ordered regimes below the critical field curves and investigate how the order parameters evolve with the field and whether it agrees

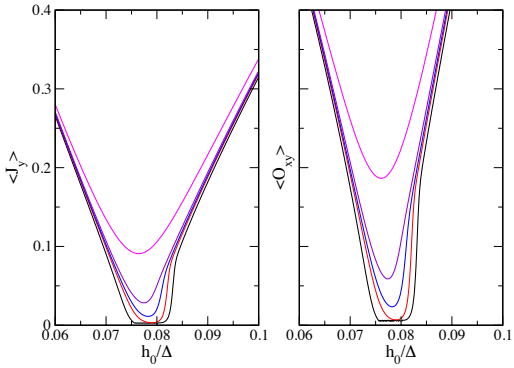

FIG. 6. Enlarged dependence of homogeneous polarization $\langle J_x\rangle$ and order parameters $\langle J_y\rangle, \langle O_{xy}\rangle$ on the applied field in the critical QCP endpoint region. Here $I_m = 0.019$ and proceeding from lower to upper curves: $I_Q = 0.01165 - 0.01168$. Both curves are asymmetric in h_0 exhibiting a first-order type jump-like behavior at the upper critical field $h^+_{0\mathrm{cr}}$.

with previous conjectures made from the instabilities approached from the disordered regime. The order parameters together with the homogeneous polarization $\langle J_z\rangle$ as obtained from the selfconsistent solution of Eq. (39) are shown in Fig 5 for the two regions. (a) with separated critical fields $h^{\pm}_{\mathrm{cr}}$ for AFM and FIQ QCP's and (b) for the coexistence case with nonzero order parameters for the whole field range. In the left part of (a) the primary AFM order parameter first induces the quadruple (red) and then at the critical AFM field $h^-_{0\mathrm{cr}}$ forces it to drop to zero again. Then a disordered sector prevails up to $h^+_{0\mathrm{cr}}$ where now a primary quadrupolar (red) order parameter reappears due to the large field- induced quadrupole matrix element of the ground state doublet. It again induces a secondary AFM order parameter. Therefore when progressing from $h^-_{0\mathrm{cr}}$ to $h^+_{0\mathrm{cr}}$ the magnetic and quadrupolar order parameter interchange their roles. In the coexistence case (b) the critical fields cease to exist and both order parameters are finite in the whole field range. However, their pronounced dip on the previous critical field positions is still prominent and should lead to rather similar thermodynamic anomalies when crossing the dip region as compared to the case (a) when the critical fields are still present. The transition region between (a) and (b) where the upper and lower QCP's merge into an endpoint is shown in Fig. 6 in an enlarged scale. The critical value for I_Q where the two critical field curves touch and merge is very close to the paramagnetic calculations in Figs. 2) and (4 that corresponds to the situation in $CeRh_2As_2$.

VIII. SUMMARY AND CONCLUSION

In this work we have investigated the possible origin of the extremely anisotropic normal state phase diagram of tetragonal $CeRh_2As_2$. We use a fully localized CEF- split 4f-electron model for the $J = 5/2$ multiplet of Ce^{3+}. We do not include the effect of Kondo screening leading to local moment reduction and heavy conduction band formation. In fact recent ARPES experimentshave suggested that $CeRh_2As_2$ is close to the localized $4f$ limit [16]. Furthermore similar examples of Ce-hexaboride and -skutterudite compounds have demonstrated that neglecting the Kondo screening may be an acceptable starting point for understanding major qualitative features of the H-T phase diagram although it may be too simple to explain the quantitive aspects.

The starting point is the conjecture that the anisotropy of this phase diagram is caused by a multipolar competition of low-field magnetic dipolar and high-field induced electric quadrupolar order parameters. This competition has been investigated analytically within a simplified quasi-quartet model valid for low fields and temperatures and numerically for the complete level scheme in the full range. We employ the RPA response function technique from the disordered side and the coupled MFA for polarization and order parameters, using effective operator technique in the ordered regime. The results of analytical and numerical approach agree in the low field regime. In the high field case the latter predicts the phase boundary in a region not yet tested experimentally.

The normal state H-T phase diagram for $\mathbf{H}_0 \parallel c$ has a the appearance of an antiferromagnet (as suggested by μSR experiments [9]) while for $\mathbf{H}_0 \parallel a$ another high field phase appears immediately after the low field phase region. Its critical temperature rises without limitation in the field range so far probed. We have shown that such behavior can be explained by the presence of easy-plane antiferromagnetic order $\langle J_y\rangle$ (moments perpendicular to $\mathbf{H}_0 \parallel a$) of Γ_5 symmetry and a field-induced quadrupolar order parameter $\langle O_{xy}\rangle$ belonging to Γ_4 type irreducible representation of C_{4v}. The FIQ phase appears because the mixing of Γ_6 excited state into the ground state $\Gamma^{(1)}_7$ where a strong matrix element (m'_Q) creates a corresponding field induced quadrupolar matrix element in the ground state (absent for zero field) which increases rapidly with applied field strength H_0. In the paramagnetic phase this means that a mixed dipolar-quadrupolar susceptibility appears such that increasing H_0 leads to a divergence for the quadrupolar RPA susceptibility at the induced ordering temperature. Likewise the coupled MF equations of homogeneous polarization $\langle J_x\rangle$ and order parameters $\langle J_y\rangle$ and $\langle O_{xy}\rangle$ in the ordered regime show that in the low field case the primary magnetic order induces the quadrupole and vice versa in the high field phase. The two QCP's where the respective order parameters vanish enclose a disordered regime. The full level scheme calculation shows that the FIQ phase will extend to high temperatures and fields similar as observed in the true Γ_8 quartet system CeB_6 although in this compound it is the coexistence of primary quadrupolar and field-induced octupolar order that drives the strong increase.

The dipolar exchange and quadrupolar effective interaction determine the ordering temperatures and the

critical fields. When the latter increases the disordered regime shrinks and vanishes at a quantum critical endpoint. This situation corresponds closely to the one observed in $CeRh_2As_2$. The interaction strengths may be characterized by dimensionless control parameters which are rather asymmetric (small for dipolar exchange and sizable but subcritical (< 1) for quadrupolar interaction). This points to the fact that the zero-field AF order is driven by the $\Gamma_7^{(1)}$ ground state moments and FIQ order by the field induced moments due to $\Gamma_7^{(1)} - \Gamma_6$ mixing. If the quadrupolar control parameter would be above critical (> 1) the quadrupolar order would likewise appear as self-induced order already at zero field as observed e.g. in the $J = \frac{7}{2}$ compound $YbRu_2Ge_2$. The near equality of the two critical fields, i.e., the stability of the quantum critical endpoint may be obtained along aline in a sizable region of the control parameter plane. The experimental verification of the proposed scenario of order parameters requires a diagnosis of the ordered phases by various means like neutron diffraction in external field, NMR experiments as well as resonant x-ray scattering. To map out the phase boundary in the high field regime with increased T_{cr} ultrasonic and resistivity measurements in pulsed fields may be suitable.

Appendix A: The C_{4v} CEF model for J = 5/2 and its multipoles

The Ce ions are located on a non-centrosymmetric lattice in layered tetragonal planes with site symmetry C_{4v}, highest rotational axis is a fourfold one. The formal charge is 3+ and Hund's rules yield a $^2F_{5/2}$ ground-state configuration. The $J = 5/2$ CEF Hamiltonian, written in Steven's operator representation [20, 24, 25] is therefore

$$\mathcal{H}_{\rm CEF} = B_2^0 O_2^0 + B_4^0 O_4^0 + B_4^4 O_4^4 \tag{A1}$$

Its eigenvalues, the CEF level energies are obtained as

$$\begin{aligned} E_{\Gamma_7^{(1)}} &= 4\left(B_2^0 - 15B_4^0\right) \\ &\quad - 6\sqrt{\left(B_2^0 + 20B_4^0\right)^2 + \left(2\sqrt{5}B_4^4\right)^2}, \\ E_{\Gamma_6} &= -8\left(B_2^0 - 15B_4^0\right), \\ E_{\Gamma_7^{(2)}} &= 4\left(B_2^0 - 15B_4^0\right) \\ &\quad + 6\sqrt{\left(B_2^0 + 20B_4^0\right)^2 + \left(2\sqrt{5}B_4^4\right)^2}, \end{aligned} \tag{A2}$$

and the corresponding eigenstates consisting of 3 Kramers doublets are given in the basis of free ion states $|M\rangle$ ($|M| \leq \frac{5}{2}$) as:

$$\begin{aligned} \left|\Gamma_7^{(1)}\right\rangle &= \cos\theta \left|\pm\frac{5}{2}\right\rangle - \sin\theta \left|\mp\frac{3}{2}\right\rangle, \\ |\Gamma_6\rangle &= \left|\pm\frac{1}{2}\right\rangle, \\ \left|\Gamma_7^{(2)}\right\rangle &= \sin\theta \left|\pm\frac{5}{2}\right\rangle + \cos\theta \left|\mp\frac{3}{2}\right\rangle, \end{aligned} \tag{A3}$$

where θ is the mixing angle of the two $\Gamma_7^{(1),(2)}$ doublets that depends on all CEF parameters according to

$$\theta \;=\; \frac{1}{2}\tan^{-1}\left(\frac{2\sqrt{5}B_4^4}{B_2^0 + 20B_4^0}\right). \tag{A4}$$

where θ is the mixing angle of the two $\Gamma_7^{(1),(2)}$ doublets that depends on all CEF parameters. Therefore the relevant matrix elements of dipolar and quadrupolar operators also depend on this angle. (We note that our definition of θ differs to Hafner et al. [5] by setting $\theta \to \pi/2 - \theta$ and we assume $B_4^4 > 0$.)

For $CeRh_2As_2$ the lowest energies are $E_{\Gamma_7^{(2)}} \equiv 0$; $E_{\Gamma_6} = 30$ K; $E_{\Gamma_7^{(1)}} = 180$ K. Therefore the lowest two doublets are well separated from the highest and form a quasi quartet whose states will be abbreviated as $\left|\Gamma_7^{(1)}\right\rangle \equiv |1\pm\rangle$ and $|\Gamma_6\rangle \equiv |2\pm\rangle$.

These states are unchanged in an external field $\mathbf{H}_0$ parallel to the c-axis. However for $\mathbf{H}_0 || a$ as described by the Zeeman term in Eq.(1) or in a molecular field consisting of Zeeman term and internal polarization and order parameters (Eq.(31)) the bare CEF states given above are further mixed. Consequently the matrix elements of multipole operators depend on θ as well on the applied or

TABLE III. Matrix elements of dipolar and quadrupolar operators, see Eqs. (A5) to (A7), in the basis of the crystal-field doublets. The primes indicate matrix elements between doublets of different symmetry, a and c label respective in-plane and out-of-plane matrix elements, Q denotes the quadrupole matrix elements. The CEF mixing angle for $CeRh_2As_2$ is $\theta = 0.346\pi$ [5], the variation with θ is shown in Fig. 7.

matrix element	CEF expression	$CeRh_2As_2$
m_{c1}	$1/2 + 2\cos 2\theta$	-0.63
m_{c2}	$1/2$	0.5
m_{a1}	$-(\sqrt{5}/2)\sin 2\theta$	-0.92
m_{a2}	$3/2$	1.5
m'_a	$-\sqrt{2}\sin\theta$	-1.25
m_{c3}	$2\sin 2\theta$	1.65
m_{a3}	$(\sqrt{5}/2)\cos 2\theta$	-0.63
m'_{a2}	$\sqrt{2}\cos\theta$	0.66
m'_Q	$\sqrt{2}(\sqrt{5}\cos\theta + 3\sin\theta)$	5.23
m'_{Q2}	$-\sqrt{2}(\sqrt{5}\sin\theta - 3\cos\theta)$	-0.83

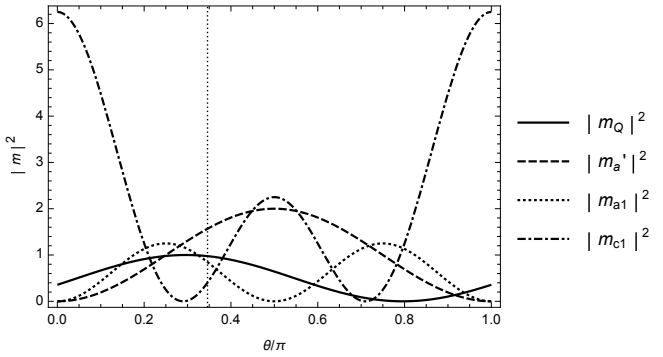

FIG. 7. Selected nonzero matrix elements between the components $|\Gamma_7^{(1)}\rangle$ and $\Gamma_6\rangle$ of the quasi-quartet for the quadrupole component O_{xy} and the dipole operators as a function of the mixing angle θ. The quadrupole matrix element (solid line) is normalized to its maximum value $|m_Q(\theta_{\max})|^2 = 28$ with $\theta_{\max} = 2\tan^{-1}\left[(1/3)\sqrt{19-2\sqrt{70}}\right] \approx 0.296\pi$. The thin vertical line denotes $\theta = 0.346\pi$ taken from experiment [5].

TABLE IV. Quadrupole operators expressed in terms of angular momentum operators

$$
\begin{aligned}
O_2^0 &= 3J_z^2 - J(J+1), \\
O_{x^2-y^2} &= J_x^2 - J_y^2 = \tfrac{1}{2}\left(J_+^2 + J_-^2\right), \\
O_{xy} &= J_xJ_y + J_yJ_x = \tfrac{1}{2\mathrm{i}}\left(J_+^2 - J_-^2\right), \\
O_{yz} &= J_yJ_z + J_zJ_y \\
&= \tfrac{1}{2\mathrm{i}}\left[\left(J_+ - J_-\right)J_z + J_z\left(J_+ - J_-\right)\right], \\
O_{zx} &= J_zJ_x + J_xJ_z \\
&= \tfrac{1}{2}\left[\left(J_+ + J_-\right)J_z + J_z\left(J_+ + J_-\right)\right].
\end{aligned}
$$

molecular fields which have to be determined selfconsistently. This evaluation of matrix elements, expectation values and susceptibilities of the multipolar operators can be done either fully numerically or semi-analytically. The former case is necessary if we consider temperatures and fields whose effective energy scale is comparable to the lowest CEF splitting energy Δ. The latter case is possible in the low-field and temperature range ($h, T \ll \Delta$) where one may restrict to the lowest quasi-quartet states as carried out in the main text.

Table III holds a compilation of the general expressions (depending on CEF mixing angle θ) of the nonzero dipolar and quadrupolar matrix elements. For completeness, Table IV holds the definitions of the quadrupole operator components in terms of the angular momentum operator components as used in this article. It is obvious that the quadrupolar matrix element m'_Q for $CeRh_2As_2$ is comparatively strong enabling the pronounced field induction of the O_{xy} quadrupole. The θ variation of (non-constant) matrix elements is shown in Fig. 7. The relevant multipole order parameters necessary for the analysis are represented by 6×6 matrices using the row and column sequence $\left\{|\Gamma_{7+}^{(1)}\rangle, |\Gamma_{7-}^{(1)}\rangle, |\Gamma_{6+}\rangle, |\Gamma_{6-}\rangle, |\Gamma_{7+}^{(2)}\rangle, |\Gamma_{7-}^{(2)}\rangle\right\}$:

dipolar Γ_5 operators:

$$
J_x = \left(\begin{array}{cccc|cc}
0 & m_{a1} & 0 & m'_a & 0 & m_{a3} \\
m_{a1} & 0 & m'_a & 0 & m_{a3} & 0 \\
0 & m'_a & 0 & m_{a2} & 0 & m'_{a2} \\
m'_a & 0 & m_{a2} & 0 & m'_{a2} & 0 \\
\hline
0 & m_{a3} & 0 & m'_{a2} & 0 & -m_{a1} \\
m_{a3} & 0 & m'_{a2} & 0 & -m_{a1} & 0
\end{array}\right)
$$

$$
J_y = \mathrm{i}\left(\begin{array}{cccc|cc}
0 & -m_{a1} & 0 & m'_a & 0 & -m_{a3} \\
m_{a1} & 0 & -m'_a & 0 & m_{a3} & 0 \\
0 & m'_a & 0 & -m_{a2} & 0 & m'_{a2} \\
-m'_a & 0 & m_{a2} & 0 & -m'_{a2} & 0 \\
\hline
0 & -m_{a3} & 0 & m'_{a2} & 0 & m_{a1} \\
m_{a3} & 0 & -m'_{a2} & 0 & -m_{a1} & 0
\end{array}\right) \tag{A5}
$$

dipolar Γ_2 operator:

$$
J_z = \left(\begin{array}{cccc|cc}
m_{c1} & 0 & 0 & 0 & m_{c3} & 0 \\
0 & -m_{c1} & 0 & 0 & 0 & -m_{c3} \\
0 & 0 & m_{c2} & 0 & 0 & 0 \\
0 & 0 & 0 & -m_{c2} & 0 & 0 \\
\hline
m_{c3} & 0 & 0 & 0 & 1-m_{c1} & 0 \\
0 & -m_{c3} & 0 & 0 & 0 & -(1-m_{c1})
\end{array}\right) \tag{A6}
$$

quadrupolar Γ_4 operator:

$$
O_{xy} = \mathrm{i}\left(\begin{array}{cccc|cc}
0 & 0 & -m'_Q & 0 & 0 & 0 \\
0 & 0 & 0 & m'_Q & 0 & 0 \\
m'_Q & 0 & 0 & 0 & -m'_{Q2} & 0 \\
0 & -m'_Q & 0 & 0 & 0 & m'_{Q2} \\
\hline
0 & 0 & m'_{Q2} & 0 & 0 & 0 \\
0 & 0 & 0 & -m'_{Q2} & 0 & 0
\end{array}\right) \tag{A7}
$$

Within the quasi-quartet model subspace the respective top left 4×4 blocks represent the multipoles with the corresponding sequence $\{|1+\rangle, |1-\rangle, |2+\rangle, |2-\rangle\}$ of states. The various matrix elements are given in terms of the CEF mixing parameter θ in Table III. Since we want to calculate the H-T phase diagram we also need these operators expressed in terms of the eigenstates in an external field corresponding to the total local Hamiltonian for each site. For $\mathbf{H} \parallel c$ there is no change while for $\mathbf{H} \parallel a$ the multipoles in quasi-quartet subspace are given in Eqs. (11) and (12) and (13).

ACKNOWLEDGMENTS

The authors thank Manuel Brando and Seunghyun Khim for helpful discussions and sharing experimental results.

[1] S. Khim, J. F. Landaeta, J. Banda, N. Bannor, M. Brando, P. M. R. Brydon, D. Hafner, R. Küchler, R. Cardoso-Gil, U. Stockert, A. P. Mackenzie, D. F. Agterberg, C. Geibel, and E. Hassinger, Field-induced transition within the superconducting state of $CeRh_2As_2$, Science **373**, 1012 (2021).

[2] J. Landaeta, P. Khanenko, D. Cavanagh, C. Geibel, S. Khim, S. Mishra, I. Sheikin, P. Brydon, D. Agterberg, M. Brando, and E. Hassinger, Field-Angle Dependence Reveals Odd-Parity Superconductivity in cerh$_2$as$_2$, Phys. Rev. X **12**, 031001 (2022).

[3] S. Ogata, S. Kitagawa, K. Kinjo, K. Ishida, M. Brando, E. Hassinger, C. Geibel, and S. Khim, Parity Transition of Spin-Singlet Superconductivity Using Sublattice Degrees of Freedom, Phys. Rev. Lett. **130**, 166001 (2023).

[4] K. Semeniuk, D. Hafner, P. Khanenko, T. Lühmann, J. Banda, J. F. Landaeta, C. Geibel, S. Khim, E. Hassinger, and M. Brando, Decoupling multiphase superconductivity from normal state ordering in cerh$_2$as$_2$, Phys. Rev. B **107**, L220504 (2023).

[5] D. Hafner, P. Khanenko, E.-O. Eljaouhari, R. Küchler, J. Banda, N. Bannor, T. Lühmann, J. Landaeta, S. Mishra, I. Sheikin, E. Hassinger, S. Khim, C. Geibel, G. Zwicknagl, and M. Brando, Possible Quadrupole Density Wave in the Superconducting Kondo Lattice $CeRh_2As_2$, Phys. Rev. X **12**, 011023 (2022).

[6] S. Mishra, Y. Liu, E. D. Bauer, F. Ronning, and S. M. Thomas, Anisotropic magnetotransport properties of the heavy-fermion superconductor $CeRh_2As_2$, Phys. Rev. B **106**, L140502 (2022).

[7] G. Chajewski and D. Kaczorowski, Discovery of Magnetic Phase Transitions in Heavy-Fermion Superconductor $CeRh_2As_2$, Phys. Rev. Lett. **132**, 076504 (2024).

[8] P. Thalmeier and G. Zwicknagl, Unconventional Superconductivity and Magnetism in Lanthanide and Actinide Intermetallic Compounds, in *Handbook on the Physics and Chemistry of Rare Earths*, Vol. 34 (Elsevier, 2004) pp. 135–287.

[9] S. Khim, O. Stockert, M. Brando, C. Geibel, C. Baines, T. J. Hicken, and H. Leutkens, preprint (2024).

[10] S. Kitagawa, M. Kibune, K. Kinjo, M. Manago, T. Taniguchi, K. Ishida, M. Brando, E. Hassinger, C. Geibel, and S. Khim, Two-Dimensional XY-Type Magnetic Properties of Locally Noncentrosymmetric Superconductor $CeRh_2As_2$, J. Phys. Soc. Jpn. **91**, 043702 (2022).

[11] D. S. Christovam, M. Ferreira-Carvalho, A. Marino, M. Sundermann, D. Takegami, A. Melendez-Sans, K. D. Tsuei, Z. Hu, S. Rößler, M. Valvidares, M. W. Haverkort, Y. Liu, E. D. Bauer, L. H. Tjeng, G. Zwicknagl, and A. Severing, Spectroscopic Evidence of Kondo-Induced Quasiquartet in $CeRh_2As_2$, Phys. Rev. Lett. **132**, 046401 (2024).

[12] R. Shiina, H. Shiba, and P. Thalmeier, Magnetic-Field Effects on Quadrupolar Ordering in a Γ_8-Quartet System CeB_6, J. Phys. Soc. Jpn. **66**, 1741 (1997).

[13] P. Thalmeier, A. Akbari, and R. Shiina, Multipolar order and excitations in rare-earth boride Kondo systems, in *Rare-Earth Borides*, edited by D. S. Inosov (Jenny Stanford Publishing, Singapore, 2021) pp. 603–677.

[14] H. S. Jeevan, C. Geibel, and Z. Hossain, Quasiquartet crystal-electric-field ground state with possible quadrupolar ordering in the tetragonal compound $YbRu_2Ge_2$, Phys. Rev. B **73**, 020407 (2006).

[15] T. Takimoto and P. Thalmeier, Theory of induced quadrupolar order in tetragonal $YbRu_2Ge_2$, Phys. Rev. B **77**, 045105 (2008).

[16] B. Chen, H. Liu, Q.-Y. Wu, C. Zhang, X.-Q. Ye, Y.-Z. Zhao, J.-J. Song, X.-Y. Tian, B.-L. Tan, Z.-T. Liu, M. Ye, Z.-H. Chen, Y.-B. Huang, D.-W. Shen, Y.-H. Yuan, J. He, Y.-X. Duan, and J.-Q. Meng, Exploring Fermi Surface Nesting and the Nature of Heavy Quasiparticles in the Spin-Triplet Superconductor Candidate $CeRh_2As_2$ (2024), arXiv:2403.14057 [cond-mat].

[17] J. Jensen and A. R. Mackintosh, *Rare Earth Magnetism: Structures and Excitations* (Clarendon Press, Oxford, 1991).

[18] G. F. Koster, J. O. Dimmock, R. G. Wheeler, and H. Statz, *Properties of the thirty-two point groups* (M.I.T. Press, Cambridge, Massachusetts, 1963).

[19] H. J. Zeiger and G. W. Pratt, *Magnetic Interactions in Solids*, International series of monographs on physics (Clarendon Press, Oxford, 1973).

[20] Y. Kuramoto, H. Kusunose, and A. Kiss, Multipole Orders and Fluctuations in Strongly Correlated Electron Systems, J. Phys. Soc. Jpn. **78**, 072001 (2009).

[21] E. W. Rosenberg, J.-H. Chu, J. P. C. Ruff, A. T. Hristov, and I. R. Fisher, Divergence of the quadrupole-strain susceptibility of the electronic nematic system $YbRu_2Ge_2$, Proceedings of the National Academy of Sciences **116**, 7232 (2019).

[22] R. Shiina, Remark on High-Field Phase Diagram of CeB_6, J. Phys. Soc. Jpn. **71**, 2257 (2002).

[23] R. G. Goodrich, D. P. Young, D. Hall, L. Balicas, Z. Fisk, N. Harrison, J. Betts, A. Migliori, F. M. Woodward, and J. W. Lynn, Extension of the temperature-magnetic field phase diagram of CeB_6, Phys. Rev. B **69**, 054415 (2004).

[24] M. T. Hutchings, Point-Charge Calculations of Energy Levels of Magnetic Ions in Crystalline Electric Fields, in *Solid State Physics*, Vol. 16, edited by F. Seitz and D. Turnbull (Academic Press, 1964) pp. 227–273.

[25] K. R. Lea, M. J. M. Leask, and W. P. Wolf, The raising of angular momentum degeneracy of f-Electron terms by cubic crystal fields, J. Phys. Chem. Sol. **23**, 1381 (1962).